



## Magnetic instabilities in Nb<sub>3</sub>Sn strands

V.V. Kashikhin, A.V. Zlobin

### 1. Introduction

Flux jumps in superconducting filaments release fair amounts of energy that under certain conditions may bring the superconductor to normal state that can be a cause of premature quenches in the Fermilab shell and racetrack type magnets [1]. That preliminary analysis based on the strand magnetization measurements did not account for the transport current in the filaments and corresponding reduction of the filament magnetization.

This note is an attempt to analyze the problem using a different approach, similar to the described in [2] for calculation of the strand adiabatic stability. The goal was to determine the strand short sample limit as a function of field, using basic input parameters, like the strand diameter and effective filament size, strand chemical decomposition and specific heat.

### 2. Model for adiabatic stability calculation

#### 2.1. Basic description

The calculations were based on the *critical state model* [3], according to which there are only two possible cases for current flow in a hard superconductor – the current density is either zero or equal to the critical current density  $J_c$  at given field and temperature. Filed changes inside the superconductor start from its surface.

#### 2.2. Current and field distributions

The field inside the superconducting filament carrying transport current and exposed to external magnetic field  $B_{ext}$  is determined by a superposition of the external field, the self field from the transport current and the field generated by the persistent currents, as shown in Figure 1-*a*). In case of the fully penetrated filament, the whole area is spanned by a combination of the transport and persistent currents with density  $J_c$  and non-zero magnetic field. If the external field is smaller than the penetration field, depending on the value of the transport current there may be a current and field free region in the center of the filament, as shown in Figure 1-*b*).

The field distribution inside a filament was calculated for current-carrying ellipses with the same origin and opposite current signs for the transport current and with shifted origins and opposite current signs for the persistent current [4]. Figure 2 presents typical field distributions from the transport and persistent currents along horizontal (i.e. normal to the external field) axis of the filament and their superposition.

Density of magnetic field energy stored in the magnetic field can be found as:

$$\omega = \frac{\vec{B} \cdot \vec{H}}{2} \text{ or } \omega = \frac{\vec{A} \cdot \vec{J}}{2}.$$

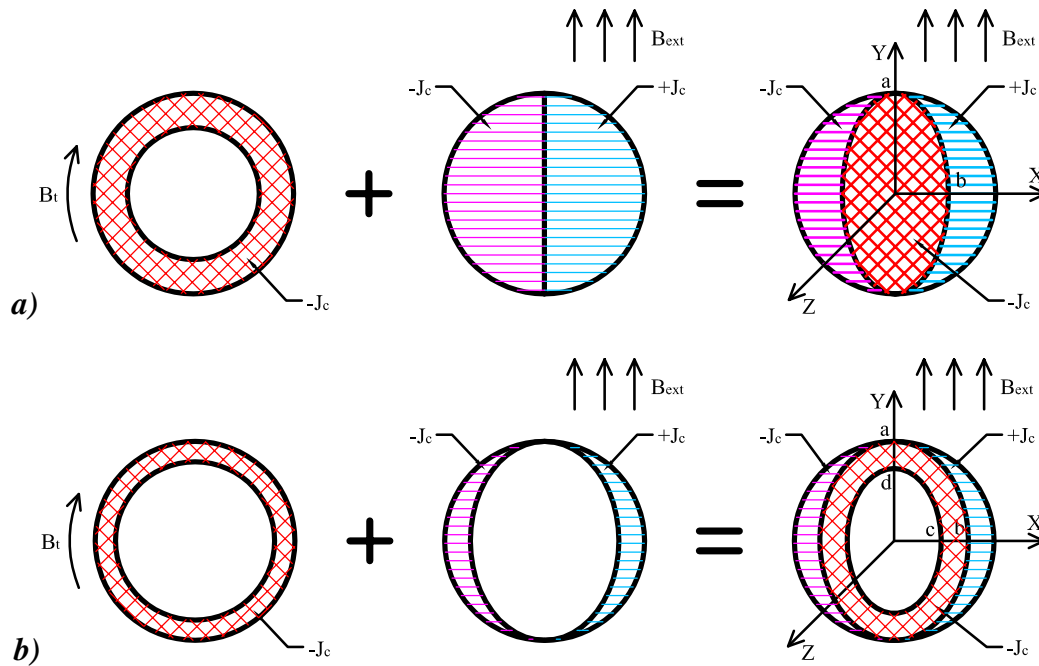


Figure 1. Combination of the transport and persistent currents inside a filament. Full penetration *a)* and partial penetration *b)*.

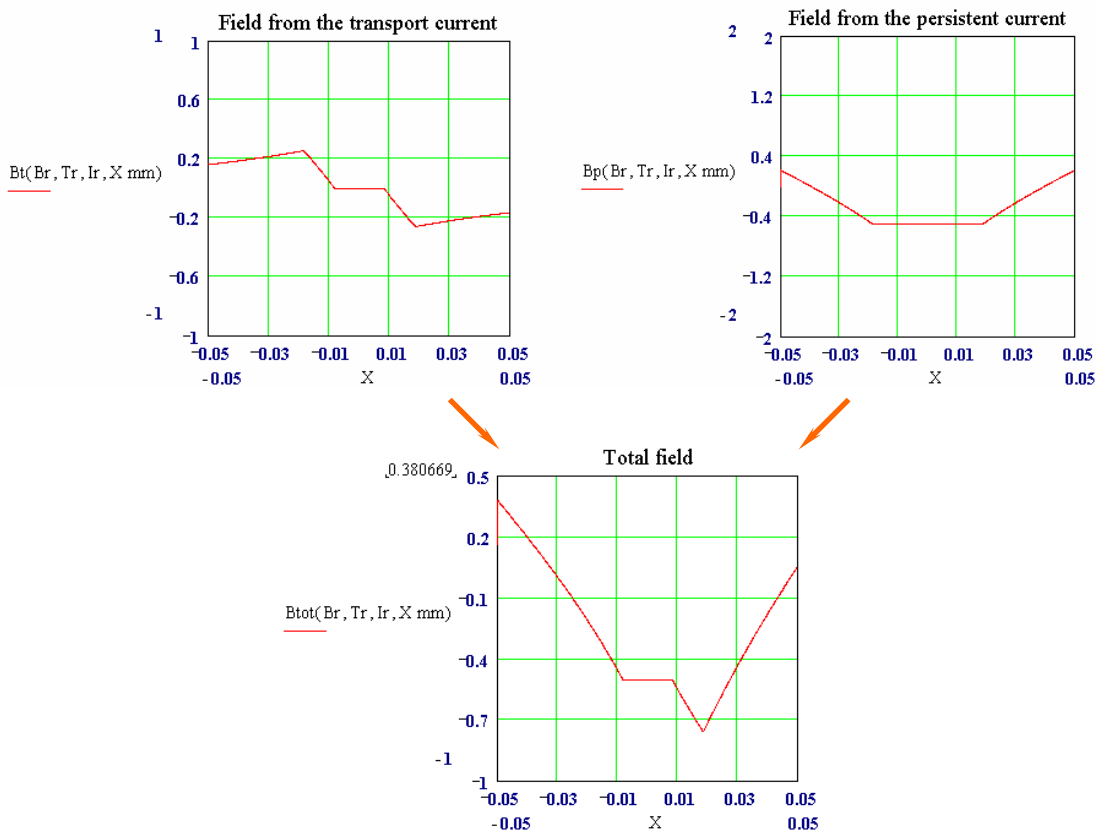


Figure 2. Typical field distribution inside a filament.

The former expression was used in [1] to evaluate energy dissipations from measured jumps of the strand magnetization. The assumption of constant current density in a filament makes it more convenient to use the latter expression, where the vector potential in 2D case has only one component yielding the integral of magnetic field over the filament axis.

### 2.3 Energy depositions due to flux change

Specifying increment of the temperature rise as  $\Delta T$ , one can find difference in magnetic field distribution inside the filament (Figure 3) and relevant decrement of the energy density, corresponding to the energy dissipation in form of heat (Figure 4). At some temperature increment, the superconductor enters the normal state that is shown as an abrupt change in the energy dissipation.

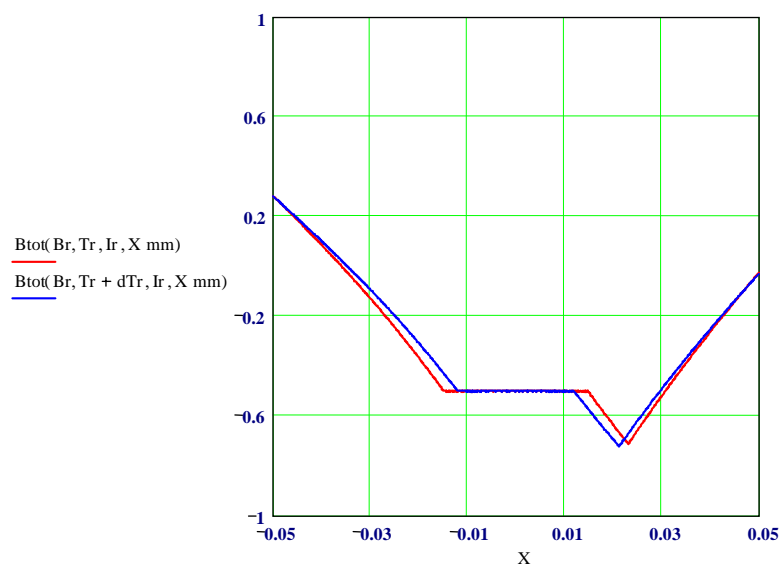


Figure 3. Typical field profile change due to a temperature rise by  $\Delta T$ .

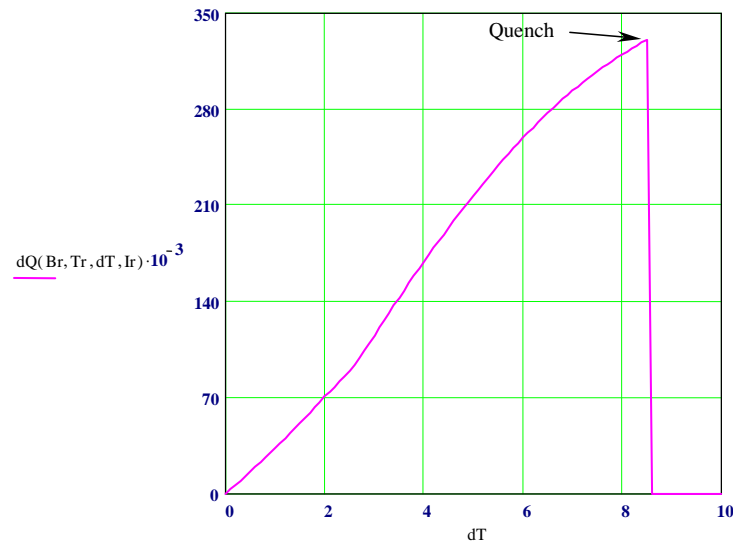


Figure 4. Typical heat dissipations due to a temperature rise by  $\Delta T$ .

### 2.4 Critical current parameterization

The critical current density of Nb<sub>3</sub>Sn was parameterized according to [5] with an additional terms responsible for the self-field correction at low fields. Figure 5 shows the parameterization before and after correction.

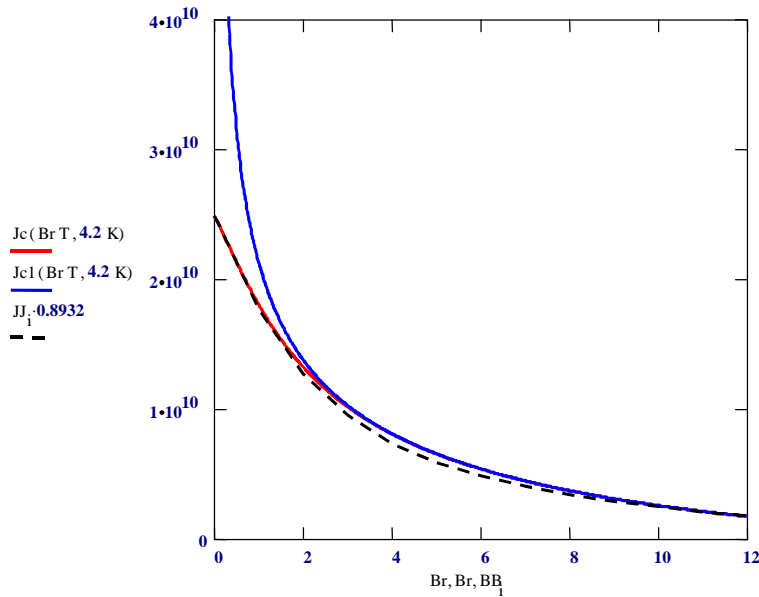


Figure 5. Critical current density parameterization.

### 2.5. Strand enthalpy

Specific heat of Nb<sub>3</sub>Sn composite strand is presented in Figure 6. In order to determine how much heat can be absorbed in the strand at a given temperature, the specific heat curve should be integrated over the temperature range of interest.

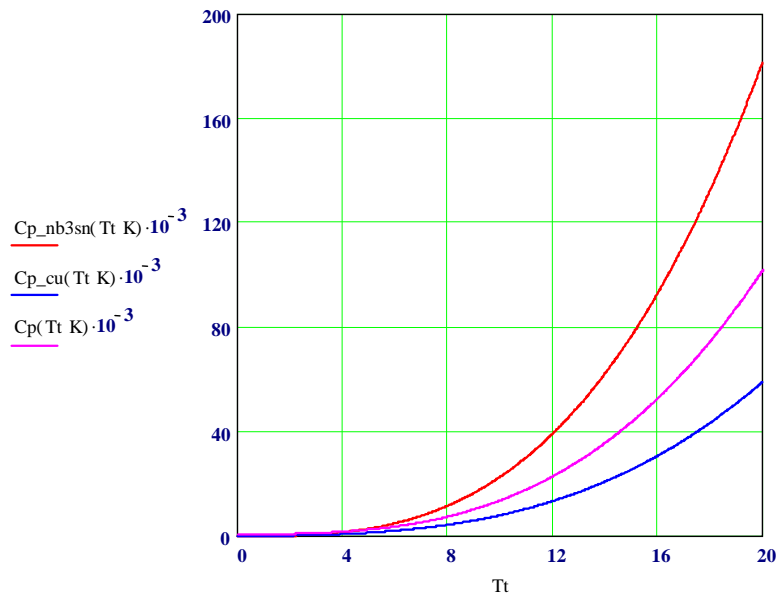


Figure 6. Specific heat of the composite Nb<sub>3</sub>Sn strand. Units on horizontal and vertical axes are respectively [mJ/cm<sup>3</sup>K] and [K].

## 2.6. Adiabatic stability criterion

Suppose there is an infinitely small amount of heat  $\Delta Q_1$ , deposited in the strand from some external source. The strand temperature will rise by  $\Delta T_1$ , according to the enthalpy curve. This temperature change will reduce the strand critical current and thus change the field profile that will in turn generate heat deposition  $\Delta Q_2$ , which will rise the temperature by  $\Delta T_2$  and so on. This avalanche-like process will continue until either the strand temperature reach the critical temperature at a given external field and transport current (Figure 7) or the strand enthalpy will exceed the heat deposition (Figure 8). In the first case, an infinitely small temperature variation leads to the strand quench, when in the second case the strand temperature rise will stop before the quench conditions develop. Then the strand adiabatic stability criteria can be defined as a curve, where each point corresponds to the case when the stable equilibrium and quench conditions are reached together.

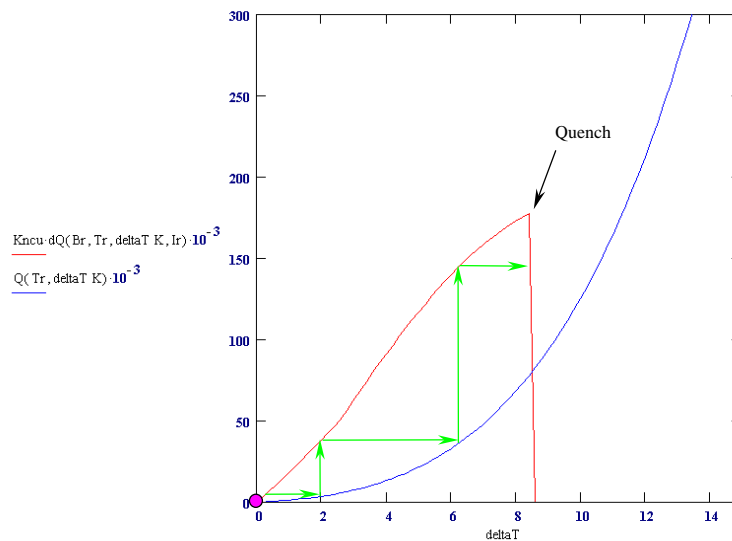


Figure 7. Adiabatic instability – quench happens before the stability point is reached.

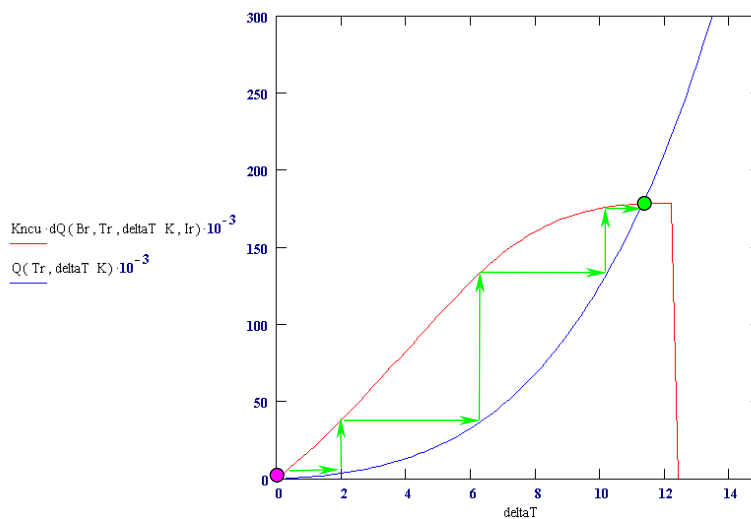


Figure 8. Adiabatic stability point is reached without a quench.

The algorithm of finding consequences of a flux jump can be described as follows:

- $B(B_{ext}, T, I, X)$  - field distribution inside a filament;
- $\Delta W(B_{ext}, T, \Delta T, I)$  - energy increment due to a temperature variation;
- $\Delta Q(T, \Delta T)$  - strand enthalpy due to a temperature variation;
- $\Delta W(B_{ext}, T, \Delta T, I) > \Delta Q(T, \Delta T)$  - determine if there is an instability;
- $\Delta T_S(\Delta W = \Delta Q)$  - determining the temperature increment of stable equilibrium;
- $\Delta W(B_{ext}, T, \Delta T_S, I) > \Delta Q(T, \Delta T_S)$  - determine if instability causes transition to the normal state;

### 3. Strand critical and quench currents

The adiabatic stability was analyzed for 1.0-mm and 0.7-mm MJR strands supplied by OST. The input parameters used in the calculations are shown in Table 1. The strand critical currents calculated in 0-12 T field region are presented in Figure 9 and Figure 10 along with the load lines of the cosine-theta and racetrack magnets.

Table 1. MJR strand parameters.

Parameter	Unit	0.7-mm strand	1.0-mm strand
Strand diameter	mm	0.7	1.0
Effective filament radius	mm	0.039	0.055
Cu to non-Cu ratio		0.85	0.85
Nb <sub>3</sub> Sn fraction in the non-Cu		0.64	0.64
Reference critical current	A/mm <sup>2</sup>	1786	1786
Reference field	T	12	12
Reference temperature	K	4.2	4.2
Upper critical field	T	28	28
Upper critical temperature	K	18	18

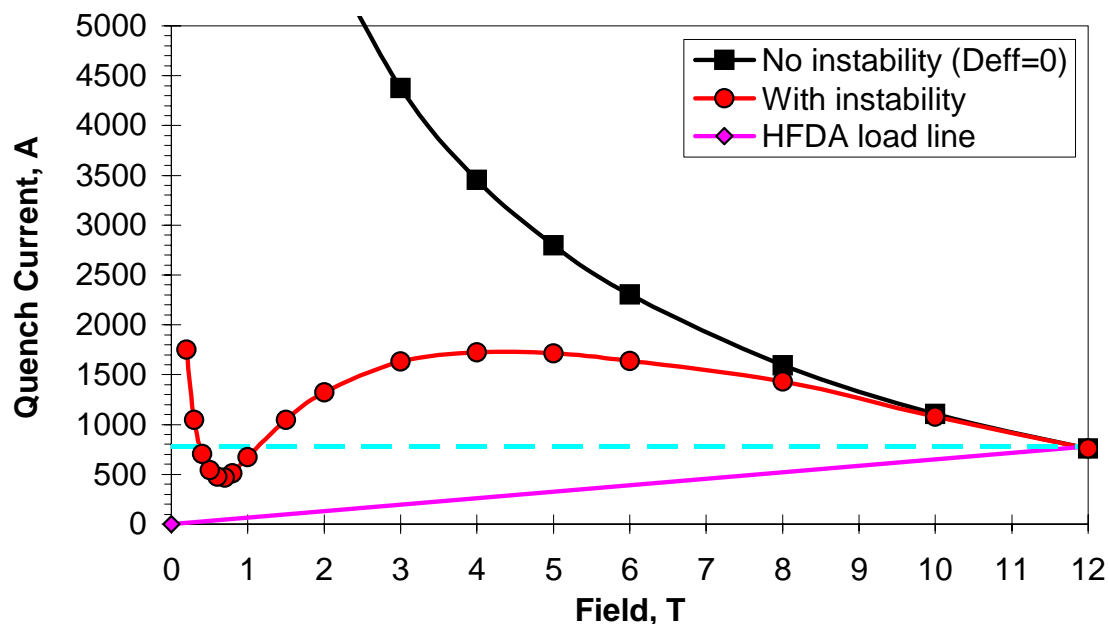


Figure 9. Critical current of 1-mm MJR strand.

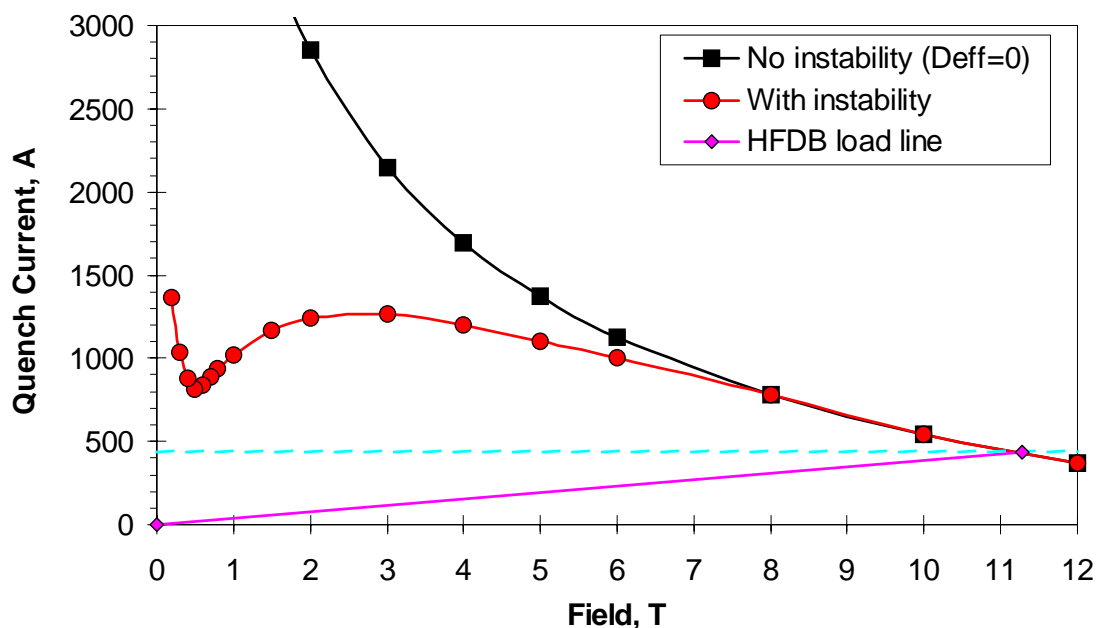


Figure 10. Critical current of 0.7-mm MJR strand.

The critical current curves have well pronounced minimum at  $\sim 0.5$  T field due to peculiarity of the field distribution inside the filaments. This minimum is 40% lower than the nominal quench current (based on the short sample measurements at high fields) of the cosine theta magnet that may be the reason of the magnet quenches at 12-14 kA. However, in case of the racetrack magnet, the minimum is 46% above the nominal quench current that does not explain premature quenches in the short models.

## Conclusion

A model for analysis of adiabatic instabilities in superconducting strands was built and tested with two strand types used in Fermilab cosine-theta and racetrack magnets. It was found that calculated quench current has a good correlation with the one measured in the cosine-theta short models. The model suggests that the reason of premature quenches in the racetrack models is not in the strand magnetic instabilities (alone).

More work needs to be done on verifying the model with the strand measurements and analyzing effects of non-uniform transport current distribution within a strand, heat transfer and current sharing between adjacent filaments and external cooling by liquid helium.

## References:

- [1] V.V. Kashikhin, "Flux jumps in  $Nb_3Sn$  magnets," Fermilab note, TD-03-005.
- [2] M.N. Wilson, Superconducting magnets, Clarendon Press, Oxford, 1983.
- [3] C.P. Bean, "Magnetization of high-field superconductors," Review of Modern Physics, Vol. 36, No. 1, 1964, pp. 31-39.

- [4] H. Brechna, Superconducting magnet systems, Springer, Berlin, 1973.
- [5] L.T. Summers, M.W. Guinan, J.R. Miller, P.A. Hahn, "A model for the prediction of Nb<sub>3</sub>Sn critical current as a function of field, temperature, strain and radiation damage," IEEE Trans. Magnetics, 27 (2): 2041-2044, 1991.